World Academy of Science, Engineering and Technology
International Journal of Civil and Environmental Engineering
Vol:7, No:9, 2013

Study Punching Shear of Steel Fiber Reinforced Self Compacting Concrete Slabs by Nonlinear Analysis

Khaled S. Ragab

***Abstract*—**This paper deals with behavior and capacity of punching shear force for flat slabs produced from steel fiber reinforced self compacting concrete (SFRSCC) by application nonlinear finite element method. Nonlinear finite element analysis on nine slab specimens was achieved by using ANSYS software. A general description of the finite element method, theoretical modeling of concrete and reinforcement are presented. The nonlinear finite element analysis program ANSYS is utilized owing to its capabilities to predict either the response of reinforced concrete slabs in the post elastic range or the ultimate strength of a flat slabs produced from steel fiber reinforced self compacting concrete (SFRSCC). In order to verify the analytical model used in this research using test results of the experimental data, the finite element analysis were performed then a parametric study of the effect ratio of flexural reinforcement, ratio of the upper reinforcement, and volume fraction of steel fibers were investigated. A comparison between the experimental results and those predicted by the existing models are presented. Results and conclusions may be useful for designers, have been raised, and represented.

***Keywords*—**Nonlinear FEM, Punching shear behavior, Flat slabs and Steel fiber reinforced self compacting concrete (SFRSCC).

I. Introduction

FLAT-PLATE slab system is widely adopted by engineers as it provides many advantages such as reduction of floor height, more spatial planning due to no beams present. These advantages further results in reduction in material cost. In the flat plate slab-slab connection is always subjected to combination of high bending moments and shear stresses, which develop a punching, shear failure. This failure is undesirable as it occurs without warning and may lead to progressive collapse of slab. Due to large tensile stresses, the potential diagonal crack in the form of truncated cone or pyramid is formed around the slab. The failure surface extends from bottom of the slab at the support, diagonally upward up to the top surface. The angle of inclination with the horizontal depends on slab reinforcement. Hence, designing of flat-plate requires a special attention for both strength and ductility when punching shear being consider. The punching shear capacity of the slab-slab connection is affected by the size of the slab, the depth of slab, flexural reinforcement and compressive strength of slab etc. Punching shear failure of slabs is usually sudden and leads to progressive failure of flat plate structures; therefore, caution is needed in the design of slabs and attention should be given to avoid the sudden failure conditions. Punching shear of slabs were interested by several researches and several experimental investigations were conducted to increase the punching shear strength of slabs by using steel fiber reinforced concrete or high strength concrete or concrete polymer composite(4). Recently, new technique using steel fibers to improve the punching shear resistance and cracking control of slab-slab connections has been proven to give good results (Alexander and Simmonds 1992 [2]; Theodorakopoulos and Swamy 1993 [3]; Harajli et al. 1995[5]; McHarg et al. 2000 [6], Naaman et al. 2007 [8]; Cheng and Montesinos 2010a [25]). Moreover, steel fibers also indicate high effectiveness in structures sustained lateral loads i.e. seismic because of their ability to absorb energy dissipation of the structures (Megally and Ghali 2000 [11]; Cheng and Montesinos 2010b [11]). The newest construction material (technique) which can be used in such cases are moderate or high strength self compacted concrete rather than using conventional shear reinforcement to increase capacity of flat slab. Self-compacting concrete (SCC) was developed in Japan in the late 1980's and allows concrete to be placed fully compacted without segregation and with no additional energy (vibration). The main objective of this study is to investigate nonlinear analysis for capacity of steel fiber reinforced self compacting concrete (SFRSCC) slabs under punching shear force, in which, a total of neon small-scale flat slabs were analyzed.

Modeling the constitutive law of the punching shear behavior of steel fiber reinforced self compacting concrete (SFRSCC) slabs based on the empirical approach can sometimes be inaccurate or limited to a narrow range of available experimental data. The tests are also very expensive and sometimes time consuming. The applicability of the test data mainly depends on the accuracy of the test apparatus and the supporting instruments implemented during the test. Hence, it is deemed necessary to have another option of modeling the punching shear behavior of steel fiber reinforced self compacting concrete (SFRSCC) slabs without deploying an empirical approach in the modeling. One of the suitable software that can be utilized to describe the actual nonlinear behavior of the punching shear behavior of steel fiber reinforced self compacting concrete (SFRSCC) slabs is ANSYS [1]. This is because ANSYS is capable of analyzing the nonlinear behavior of a combination between 3D SOLID and LINK elements in a structure based on the finite element procedure. With this option, researchers or design engineers can confidently predict in advance the actual

Khaled S. Ragab is Associate Professor, Reinforced Concrete Research Institute, Housing & Building National Research Center, HBRC, Cairo, Egypt. (kh_ragab@yahoo.com)

behavior of various punching shear behavior of steel fiber reinforced self compacting concrete (SFRSCC) slabs not only in the linear-elastic region, but furthermore also in the nonlinear post-elastic region. The authors wish that this economical procedure can be used to provide an alternative tool for researchers or structural engineers in investigating various types of structural concrete elements in the future. In this paper, the authors propose to use ANSYS [1], which is capable of modeling the nonlinear punching shear behavior of steel fiber reinforced self compacting concrete (SFRSCC) slabs, for predicting the actual punching shear strength. A general description of the finite element method, theoretical modeling of concrete and reinforcement are presented. In order to verify the analytical model used in this research using test results of the experimental results obtained from three flat slab specimens, the finite element analysis were performed then a parametric study for six flat slabs specimens were investigated the effect ratio of flexural reinforcement, ratio of the upper reinforcement, and volume fraction of steel fibers. The punching shear strength obtained from the proposed procedure is shown to be in close agreement with the experimental results.

II. Objectives and Scope

The main objectives of this study could be summarized in the following points:

- Examining the punching shear behavior of steel fiber reinforced self compacting concrete (SFRSCC) slabs.
- Knowing better for punching shear behavior of steel fiber reinforced self compacting concrete (SFRSCC) slabs during the loading.
- Parametric study for the effect ratio of flexural reinforcement, ratio of the upper reinforcement, and volume fraction of steel fibers.
- Predicate new formula for compute the capacity of the punching shear of steel fiber reinforced self compacting concrete (SFRSCC) slabs.

Finite element models were developed to simulate the punching shear behavior of steel fiber reinforced self compacting concrete (SFRSCC) slabs from linear through nonlinear response using the ANSYS program.

III. Experimental and Analytical Program

The experimental models were constructed according to flat slab specimens as shown in Fig. 1. The specimens had tested of various punching shear behavior of steel fiber reinforced self compacting concrete (SFRSCC) slabs. Test set up and general view of flat slabs are shown in Fig. 2. The experimental program had chosen three flat slabs. These slabs are shown in Table I from S1 to S3. The specimens had square shape of dimensions 110 * 110 cm and 10 cm thickness and bottom steel was 7 Φ 10/m. The analysis carried out is conducted on nine flat slabs as shown in Table I; the parameters of study were the effect ratio of flexural reinforcement, ratio of the upper reinforcement, and volume fraction of steel fibers. All the specimens from S1 to S9 are analysis by FEM using ANSYS program. Finally, conclusions from the current research and recommendations for future studies are presented.

Fig. 1 Details of steel reinforcement and self compacting concrete

Fig. 2 General view of flat slabs and Test set up

TABLE I
CONCRETE MIX DESIGN

Slab No	Type of Mix	Mix Proportions (Kg)									Fresh test	
		Cement	Sand	Coarse aggregate		Steel fibers	FA	SF	Add.	Water (Liter)	Slump (cm)	Slump flow (cm)
				C.agg1	C.agg2							
S1	OC	350	750	550	550	-	-	-	-	175	4	-
S2	SCC	350	950	950	-	-	35	52.5	10	158	27	60
S3	SCC V_f 0.75%	350	950	950	-	58.5	35	52.5	10	171	7	60

OC: Ordinary concrete, SCC: Self compacted concrete, Vf: percentage of fiber volume fraction, FA: fly ash, SF: silica fume, and Add.: admixture.

TABLE II
THE PROGRAM FOR THE ANALYTICAL SLABS

Model by	Slab No.	Dim. bxdxt (mm)	Type of concrete	Steel Fiber volume fraction V_f (%)	Reinforcement (mm)/M		Target Comp. Str. (MPa)
					Bot.	Top	
Exp.	**S1**	110x110x10	Ordinary	---	7#10	---	30
and	**S2**	110x110x10	S.C.C	0.0	7#10	---	64
FEM	**S3**	110x110x10	S.C.C	0.75	7#10	---	55
	S4	110x110x10	S.C.C	1.0	7#10	---	55
	S5	110x110x10	S.C.C	1.5	7#10	---	55
	S6	110x110x10	S.C.C	0.75	7#8	---	55
FEM	**S7**	110x110x10	S.C.C	0.75	7#12	---	55
	S8	110x110x10	S.C.C	0.75	7#10	7#10	55
	S9	110x110x10	S.C.C	0.75	7#10	7#12	55

* S.C.C: Self compacted concrete.

A. Element Types

Extensive inelastic finite element analyses using the ANSYS program are carried out to study the behavior of the tested slabs. Two types of elements are employed to model the slabs. An eight node solid element, solid65, was used to model the concrete. The solid element has eight nodes with three degrees of freedom at each node, translation in the nodal x, y, and z directions as shown in Fig. 3. Used element is capable of plastic deformation, cracking in three orthogonal directions, and crushing. The geometry and node locations for this element type are shown in Fig. 3. The element is used to model the three-dimensional problems of solids with or without reinforcing bars. A link8 element was used to model the steel bars; two nodes are required for this element. Each node has three degrees of freedom, translation in the nodal x, y, and z directions. The element is also capable of plastic deformation (ANSYS User's Manual). The finite element mesh used in the analysis is shown in Fig. 4.

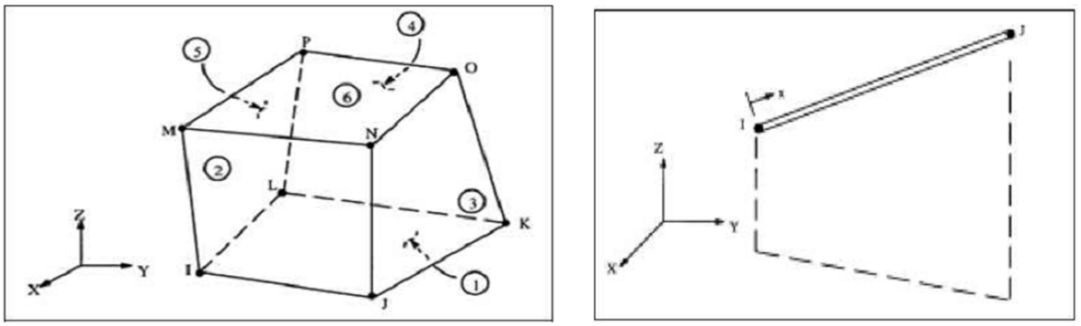

Solid 65 Link 8

Fig. 3 Element type Solid 65 and Link8

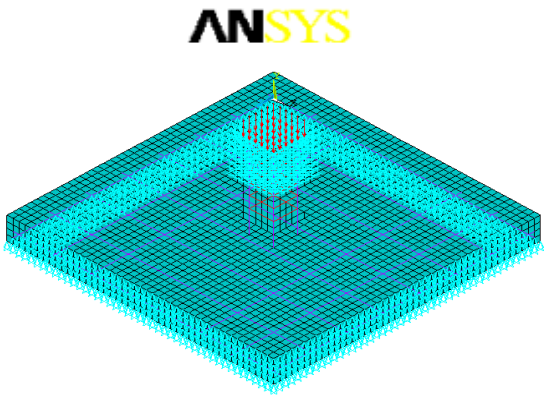

(a) Finite element mesh model

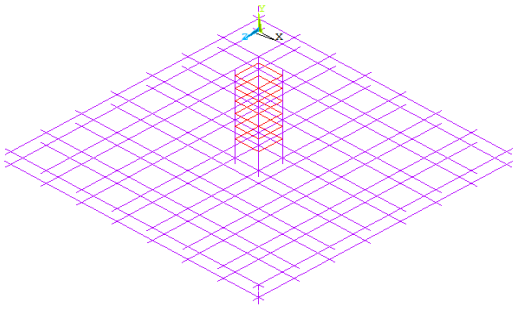

(b) Steel model for S8 before loading

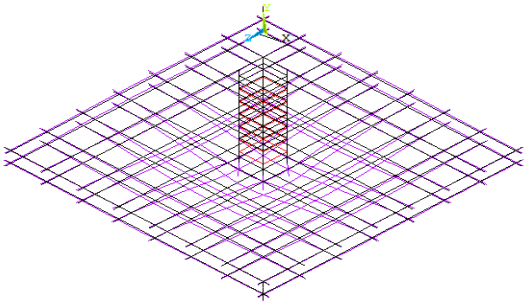

(c) Steel model for S8 after loading

Fig. 4 Finite element mesh for a typical slab model and steel model

IV. Properties of the Used Material

Normal weight concrete was used in the fabricated tested slabs. The stress-strain curve is linearly elastic up to about 30% of the maximum compressive strength. Above this point, the stress increases gradually up to the maximum compressive strength, f_{cu}, after that the curve descends into softening region, and eventually crushing failure occurs at an ultimate strain. The input data for the concrete and steel (high grade and mild steel) properties are shown in Table III.

A. Reinforced Concrete

The tested reinforced concrete slabs were cast using locally produced ordinary Portland cement, natural sand and crushed stone with a maximum size of 10 mm. The slabs were remolded after 24 hrs from casting, covered with wet burlap and stored under the laboratory conditions for 28 days before proceeding to testing stage.

1. Concrete in Compression and Tension

Development of a model for the behavior of concrete is a challenging task. Concrete is a quasi-brittle material and has different behavior in compression and tension. The tensile strength of concrete is typically 8-15% of the compressive strength. Fig. 5 shows a typical stress-strain curve for normal weight concrete. In compression, the stress-strain curve for concrete is linearly elastic up to about 30 percent of the maximum compressive strength. Above this point, the stress increases gradually up to the maximum compressive strength $\sigma_{cu.}$ After it reaches the maximum compressive strength σ_{cu}, the curve descends into a softening region, and eventually crushing failure occurs at an ultimate strain $\varepsilon_{cu.}$ In tension, the stress- strain curve for concrete is approximately linearly elastic up to the maximum tensile strength $\sigma_{tu.}$. After this point, the concrete cracks and the strength decreases gradually to zero. For concrete, ANSYS requires input data for material properties as follows: Elastic modulus (Ec), Ultimate uniaxial compressive strength (σ_{cu}), Ultimate uniaxial tensile strength (σ_{tu}), Poisson's Ratio (υ), Shear transfer coefficient (βt), and Compressive uniaxial stress-strain relationship for concrete. For the full-scale specimen tests, an effort was made to accurately estimate the actual elastic modulus of the specimens. From this work, it was noted that each experimental specimen had a slightly different elastic modulus; therefore, these values were used in the finite element modeling. From the elastic modulus obtained from test results the ultimate concrete compressive and tensile strengths for each slab model were calculated by (1), and (2), respectively (ACI 318, 2002) [7].

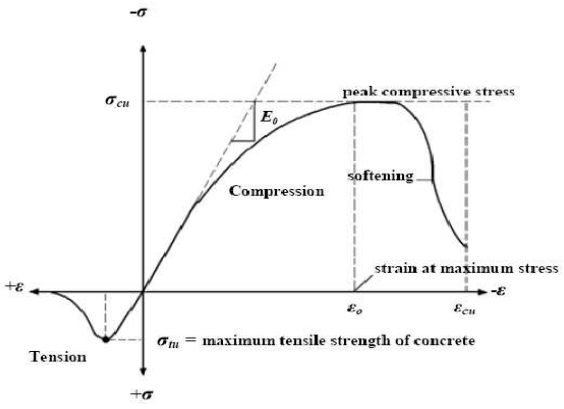

Fig. 5 Typical uniaxial compressive and tensile stress-strain curve for concrete [1]

Poisson's ratio for concrete was assumed to be 0.2 for all specimens. The shear transfer coefficient, βt, represents conditions of the crack face. The value of βt ranges from 0.0 to 1.0, where 0.0 representing a smooth crack (complete loss

of shear transfer) and 1.0 representing a rough crack (no loss of shear transfer). The value of βt used in many studies of reinforced concrete structures, however, varied between 0.05 and 0.75. A number of preliminary analysis were attempted in this study with various values for the shear transfer coefficient within this range, but convergence problems were encountered at low loads with βt less than 0.2. Therefore, the shear transfer coefficient used in this study was βt = 0.6 except in case of fiber concrete where this value will be changed based on fiber content.

2. Compressive Uniaxial Stress-Strain Relationship for Concrete

The simplified stress strain curve for slab model is constructed from six points connected by Straight lines. The curve starts at zero stress and strain. Point No. 1, at $0.3f'_c$ is calculated for the stress-strain relationship of the concrete in the linear range. Point Nos. 2, 3 and 4 are obtained from.

Equation (1), in which ε_o is calculated from (2). Point No. 5 is at ε_o and f'_c. In this study, an assumption was made of perfectly plastic behavior after Point No. 5 (William et al. 1975[1], and Meisam 2009 [10]). Fig. 6 shows the simplified compressive axial stress-strain relationship that was used in this study.

$$f = E_c \varepsilon / (1+(\varepsilon/\varepsilon_o)^2) \quad (1)$$

$$\varepsilon_o = 2 f_c' / E_c \quad (2)$$

$$E_c = f / \varepsilon \quad (3)$$

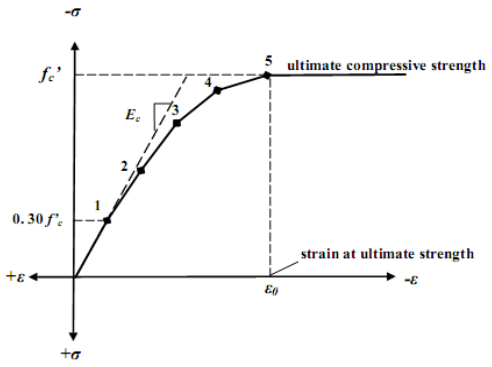

Fig. 6 Simplified compressive axial stress strain curve for concrete

3. Failure Criteria for Concrete

The model is capable of predicting failure for concrete materials. Both cracking and crushing failure modes are accounted for. The two input strength parameters; ultimate uniaxial tensile and compressive strengths, are needed to define a failure surface for the concrete. Consequently, a criterion for failure of the concrete due to a multiaxial stress state can be calculated [1]. A three-dimensional failure surface for concrete is shown in Fig. 7. The most significant nonzero principal stresses are in the x and y directions, represented by σ xp and σ yp, respectively.

Three failure surfaces are shown as projections on the σ_{xp} - σ_{yp} plane. The mode of failure is a function of the sign of σ_{zp} (principal stress in the z direction). For example, if σ_{xp} and σ_{yp} are both negative (compressive) and σ_{zp} is slightly positive (tensile), cracking would be predicted in a direction perpendicular to σ_{zp}. However, if σ_{zp} is zero or slightly negative, the material is assumed to crush [1]. In a concrete element, cracking occurs when the principal tensile stress in any direction lies outside the failure surface. After cracking, the elastic modulus of the concrete element is set to be zero in the direction parallel to the principal tensile stress direction. Crushing occurs when all principal stresses are compressive and lie outside the failure surface; subsequently, the elastic modulus is set to be zero in all directions [1], and the element effectively disappears. During this study, it was found that if the crushing capability of the concrete is turned on, the finite element slab models fail prematurely. Crushing of the concrete started to develop in elements located directly under the loads. Subsequently, adjacent concrete elements crushed within several load steps as well, significantly reducing the local stiffness. Finally, the model showed a large displacement, and the solution diverged. A pure "compression" failure of concrete is unlikely.

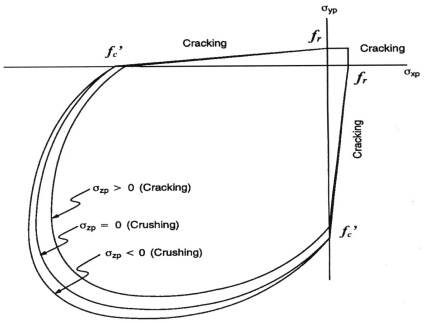

Fig. 7 3-D Failure Surface for Concrete [1]

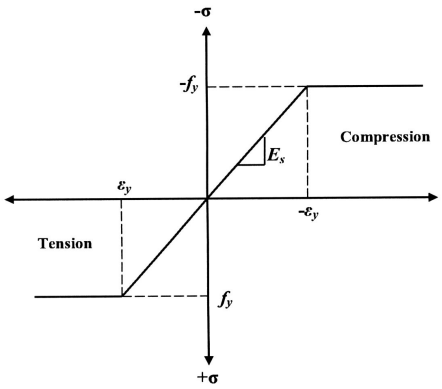

Fig. 8 Stress-Strain Curve for Steel Reinforcement

In a compression test, the specimen is subjected to a uniaxial compressive load. Secondary tensile strains induced by Poisson's effect occurs perpendicular to the load. Because

concrete is relatively weak in tension, these actually cause cracking and the eventual failure. Therefore, in this study, the crushing capability was turned off and cracking of the concrete controlled the failure of the finite element models.

B. Steel bars

The steel bars used for main longitudinal steel bars were high grade steel of 10 mm diameter. Type of steel fibers is double hooked edge, 0.6mm diameter, 30mm length, 50 and aspect ratio. Tables III shows the mechanical properties of the used materials and steel bars.

1. Fiber Reinforced Concrete

Steel fibers are a random distributed material mixed with concrete caused a significant change in concrete properties. Based on the previous statement, fibrous concrete can be represented as a new material with new elastic modulus (*Ec*), tensile strength (*ft*), and compressive strength (*fc'*). The relation between material properties for high strength concrete without fibers and that provided with fibers is obtained from the literature. These relations were used in modeling fibrous high strength concrete in ANSYS program. In addition to these properties, ANSYS program has a parameter described the crack surface βt with open and closed state. This factor plays an important role for modeling fiber reinforced concrete, and it is taken equal to 0.15 for steel fibers. The equivalent fiber reinforcement has as parameters; Young's modulus E_s = 2000000 MPa, Poisson ratio ν=0.3, and equivalent tensile strength f_s = 1500 MPa.

2. Steel Reinforcement

Steel reinforcement in the test specimens was constructed with the high strength steel (Grade 52). Properties, i.e., elastic modulus and yield stress, for the steel reinforcement used in this study follow the design material properties used for the experimental investigation. The finite element model for rebars was assumed to be an elastic-perfectly plastic material and identical in tension and compression. Poisson's ratio of 0.3 was used for the steel reinforcement in this study. Fig. 8 shows the stress-strain relationship used in this study. Material properties for the steel reinforcement for all specimens are as Table III.

TABLE III
INPUT DATA FOR THE CONCRETE, STEEL FIBERS, AND STEEL PROPERTIES

Item	Concrete	Steel Fibers	Steel (main reinf.)	Steel (stirrups)
Unit weight N/mm³	2.5e-5	7.85e-5	7.85e-5	7.85e-5
Ultimate compressive strength N/mm²	25,40	--	--	--
Tensile strength N/mm²	2.20,3.5	150	360	250
Elastic modulus N/mm²	2.4e4,2.8e4	2.0 e5	2.0 e5	2.0 e5
Poisson ratio	0.20	0.30	0.30	0.30
Shear modulus N/mm²	10.0e3,11.0e3	--	--	--

V. ELEMENT MESHING

After preparing all the input data of material and geometrical properties, the slab models were divided into small cubical elements. The meshing results of all slab specimens used for model validation are shown in Fig. 4. For slabs reinforced, it is worthwhile to notice that the meshing was created according to the locations of reinforcing bars, either the longitudinal or transverse reinforcement, as well as the slab specimen cross-sectional perimeter. By using sharing nodes option in ANSYS [1], SOLID65 and LINK8 elements can be interconnected one to another forming a single solid slab model which capable of simulating the actual behavior of R.C. slab.

A. Loading Procedure

The analytical investigation carried out here is conducted on nine-RC slabs. All slabs at a plane of support location, the degrees of freedom for all the nodes of the solid65 elements were held at zero. To apply the axial load on the top of the slab specimen, an axial pressure was implemented over the entire top surface of the slab-slab model in the ANSYS software. The axial pressure can be simulated using the ANSYS load step option [1].

B. Nonlinear Solution

In nonlinear analysis, the total load applied to a finite element model is divided into a series of load increments called load steps. At the completion of each incremental solution, the stiffness matrix is adjusted to reflect nonlinear changes in structural stiffness before proceeding to the next load increment. The ANSYS program uses Newton-Raphson equilibrium iterations for updating the model stiffness. Newton-Raphson equilibrium iterations provide convergence at the end of each load increment within tolerance limits. Fig. 9 shows the use of the Newton- Raphson approach in a single degree of freedom nonlinear analysis. Prior to each solution, the Newton-Raphson approach assesses the out-of-

balance load vector, which is the difference between the restoring forces (the loads corresponding to the element stresses) and the applied loads. Subsequently, the program carries out a linear solution, using the out-of-balance loads, and checks for convergence. If convergence criteria are not satisfied, the out-of-balance load vector is re-evaluated, the stiffness matrix is updated, and a new solution is attained. This iterative procedure is continued until the problem converges is achieved [1].

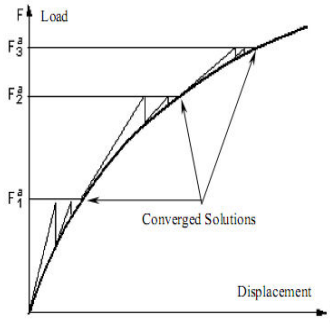

Fig. 9 Newton-Raphson iterative solution (3 load increments)

VI. Test Results and Discussion

The parametric studies included in this investigation are the effect of ratio of flexural reinforcement, ratio of the upper reinforcement, and volume fraction of steel fibers. Table IV shows the analytically and the experimental results of the ultimate loads, vertical displacements and compressive stress of concrete, respectively.

A.Load–Vertical Concrete Strain Relationship for Experimental and FEM Results

The experimental and FEM results for the load versus vertical concrete displacements relationships for slabs S1 to S3 are shown in Fig. from 10 to 13 while Table IV summarizes the test results for all slabs. The ultimate load is defined as the maximum recorded load measured during test for each slab. Table IV, indicated that, for slab S1, the experimental result for the ultimate load was recorded 219.0 kN and the corresponding vertical concrete displacement 20.0mm. When using self compacted concrete with Vf% from steel fibers equal to 0%, and 0,75% for slabs S2 and S3 the experimental results for the ultimate loads were recorded 270/0 and 313.0 kN respectively, and the corresponding vertical concrete displacements 60 and 13.4mm respectively. The FEM results for slabs S1, S2, and S3 the ultimate loads were recorded 225.0, 322.5, and 360.0 kN respectively, and the corresponding vertical concrete displacements 16.2, 58.9, and 13.1mm respectively. Table IV, indicated that, for slabs S1, S2, and S3, the difference between the FEM results and the experimental results for the ultimate loads were recorded 1.027, 1.194 ,and 1.150 respectively, and the corresponding vertical concrete displacements 0.80, 0.98 ,and 0.98 respectively. The par chart in Fig. 13 shows the difference between experimental and FEM results for S1, S2, and S3. This chart shows that the theoretical results from Finite Element Analysis indicate in general a good agreement with the experimental values.

B.Discussions of the Results

1. Effect of the Percentage of Volume Fraction from Steel Fibers V_f%.

Fig. 14 shows the load-vertical displacement of slabs S2, S3, S4, and S5; increasing percentage of volume fraction from steel fibers V_f% leads to increase the ultimate load with percentage equal to 15% for V_f% up to 0.75% and decrease the ultimate load for V_f% greater than 0.75% .

TABLE IV
Results of Tested Slabs

Model by		Slab No.	F_{cu} (MPa)	Exp. Results		FEM Results			Difference %		
				$P_{ultimate}$ (kN)	VL. Disp. (mm)	Peak stresses (MPa)	$P_{ultimate}$ (kN)	VL. Disp. (mm)	Peak stresses	$P_{ultimate}$	VL. Disp.
Exp. and FEM	Control	S1	30	219.0	20.0	26.8	225.0	16.2	0.90	1.027	0.80
		S2	64	270.0	60.0	61.0	322.5	58.9	0.95	1.194	0.98
		S3	55	313.0	13.4	52.0	360.0	13.1	0.95	1.150	0.98
FEM	S.F. volume fraction V_f (%)	S4	55	---	---	52.0	270.0	5.3	0.95	---	---
		S5	55	---	---	52.0	315.0	4.8	0.95	---	---
	Bot. Rft.	S6	55	---	---	53.0	281.3	7.9	0.96	---	---
		S7	55	---	---	54.0	371.3	13.0	0.98	---	---
	Top Rft.	S8	55	---	---	54.0	382.5	19.5	0.98	---	---
		S9	55	---	---	52.0	427.5	24.7	0.95	---	---

* S.F: Steel fiber.

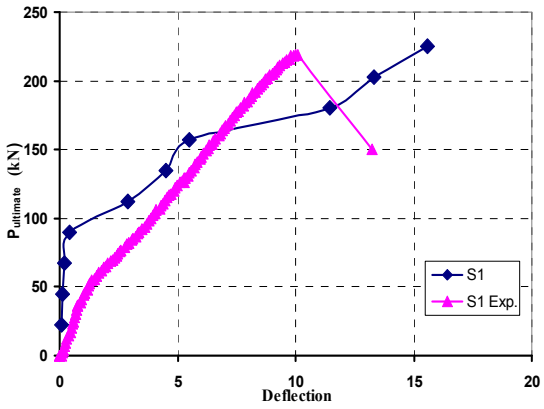

Fig. 10 Comparison between S1 Exp. and F.E.M

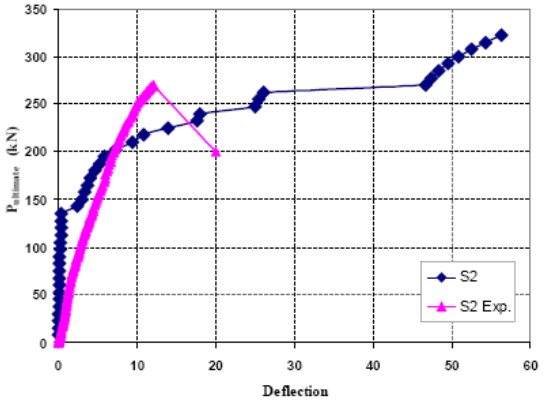

Fig. 11 Comparison between S2 Exp. and F.E.M

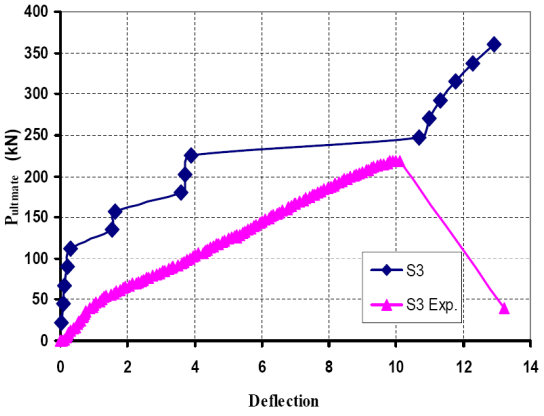

Fig. 12 Comparison between S3 Exp. and F.E.M

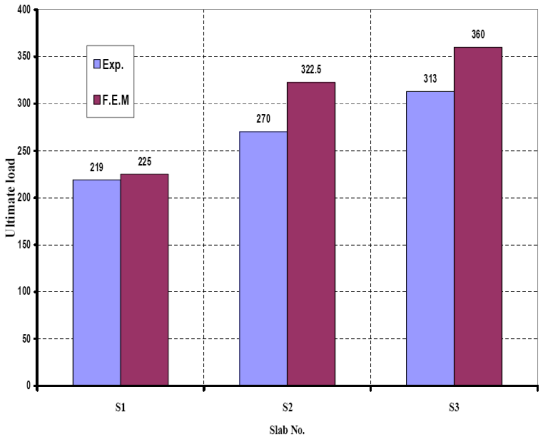

Fig. 13 Comparison between S1, S2, and S3 Exp. and F.E.M

From Table IV, it can be seen that, the ultimate load, and corresponding vertical displacement of S3, S4, and S5 are 360.0 & 270.0 & 315.0 and 13.1 & 5.3 & 4.8mm respectively. Par Chart in Fig. 17 shows that the increasing of V_f% up to 0.75% leads to increase the ultimate load of tested slabs and decrease the ultimate load for V_f% greater than 0.75%. This phenomenon appears because addition of steel fibers V_f% greater than 0.75% to self compacted concrete convert the failure to brittle failure. Also from Table IV, shows that the vertical displacement for S5 is lower than slab S3 and S4 because the increasing of percentage of volume fraction from steel fibers V_f% can significantly enhance and inhibit the initiation and growth of cracks.

2.Effect of flexural reinforcement (lower steel, tension steel)

From Table IV, it can be seen that, ultimate loads, and corresponding vertical displacement of S3, S6 and S7 are (360.0 & 281.3 & 371.3kN) and (13.1 & 7.9 & 13.0mm) respectively. Fig. 15 shows the load-displacement of slabs S3, and S7; increasing of flexural reinforcement with percentage 40% has slightly effect on the behavior of slab where increase on the ultimate load slab with percentage 3%. This increase reaches to 25% between S3 and S6 because flexural effect taking into consideration. Par Chart in Fig. 17 shows slightly effect on the ultimate loads for slabs S3 and S7.

3. Effect of Upper Steel (Compression Steel)

It can be seen from Table IV that, ultimate loads, and corresponding vertical displacement of S3, S8 and S9 are (360.0 & 381.5 & 427.5kN) and (13.1 & 19.5 & 24.7mm) respectively. Fig. 16 shows the load-displacement of slabs S3, and S7; increasing of upper steel with percentage 40% has significant effect on the behavior of slab where increase on the ultimate load slab with percentage 10%. This phenomenon appears because the upper steel (compression steel) can significantly enhance and inhibit the initiation of punching cracks. Par Chart in Fig. 17 shows this effect on the ultimate loads for slabs S8 and S9.

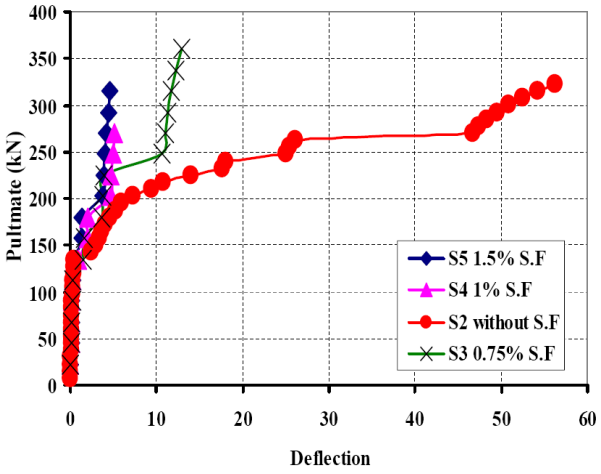

Fig. 14 Effect of volume fraction of steel fibers V_f%

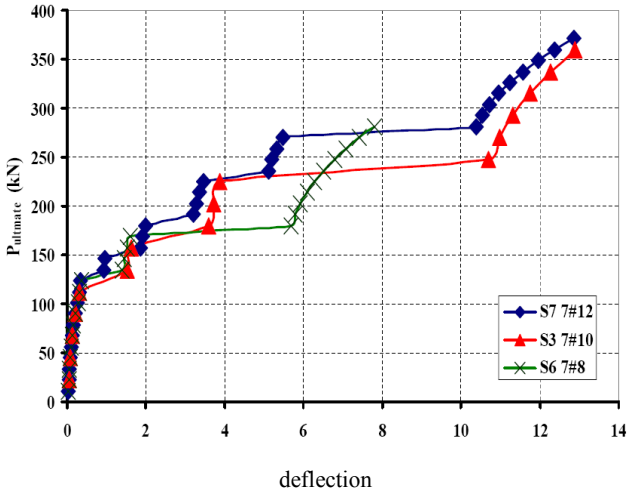

Fig. 15 Effect of flexural reinforcement (lower steel)

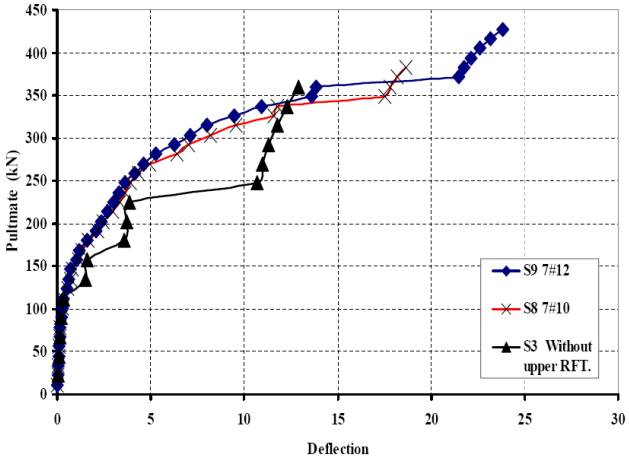

Fig. 16 Effect of upper steel(compression steel)

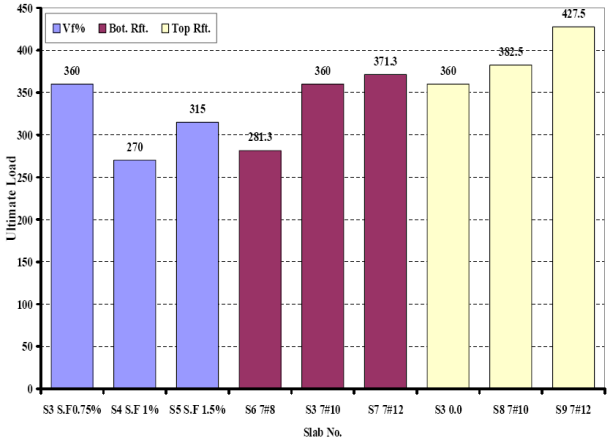

Fig. 17 Effect of flexural reinforcement (lower steel), upper steel, and volume fraction of steel fibers V_f%

VII. Stress Distribution

Fig. 19 shows the cracks occurred at the edge of the bottom face of slab which obtained from experimental. It is clear, that this cracks confirmed with the shape of the maximum intensity stresses at bottom face obtained from FEM as shown in Fig. 20. Also, Fig. 21 and 22 show the crushing of slab concrete which occurred at maximum intensity of stresses at the top face of slab and occurred around the column.

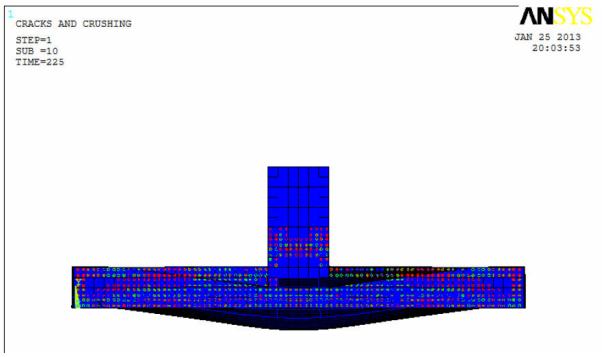

Fig. 18 Side View shape of crushing at top face and cracks at bottom face from FEM

Fig. 19 Shape of cracks at bottom face for S1 Exp. (crack mode)

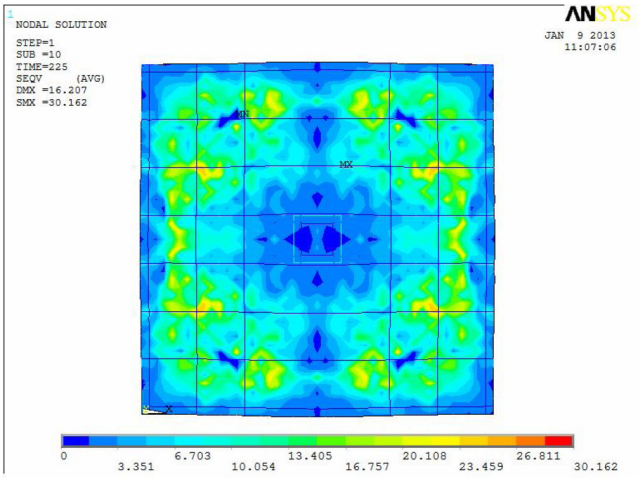

Fig. 20 Shape of max. intensity of stresses at bottom face for S1 from FEM

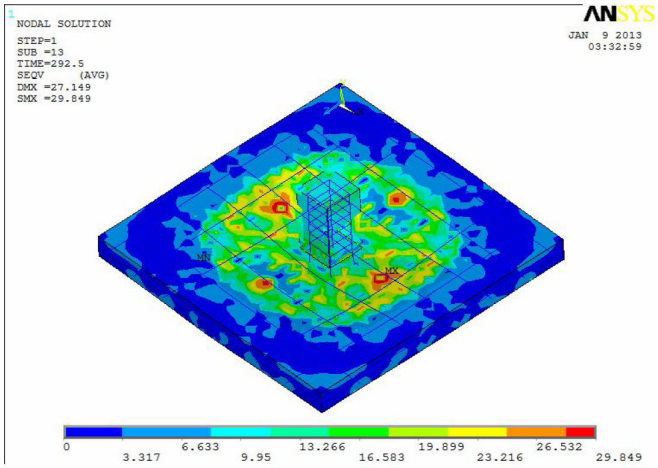

Fig. 21 3D for Shape of max. intensity of stresses at top face for S1 from FEM

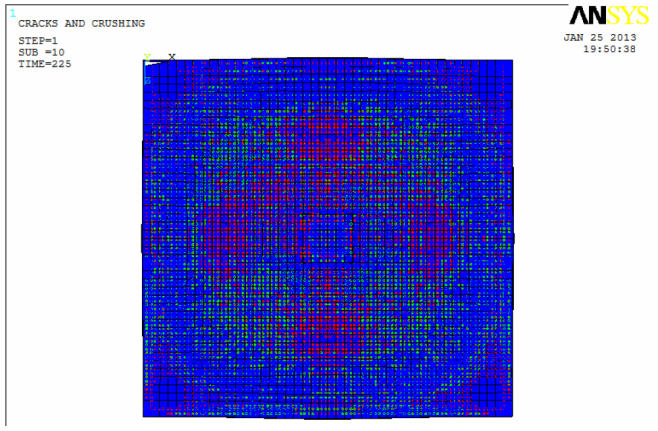

Fig. 22 Shape of crushing at top face for S1 from FEM

VIII. Evaluation of Punching Shear Resistance

A. Comparison of Results to Other Models

In this section a series of models and equations will be presented from the work of other researchers and compared to the results obtained during testing. The equations are first presented in this section and then compared to the results obtained during testing in section VIII-B.

Shaaban and Gesund Equation

Shaaban and Gesund 1994[4] studied the effects of steel fibers on the punching shear strength of reinforced concrete slabs, specifically whether the addition of steel fibers significantly enhanced punching shear capacity. Thirteen slabs with varying fiber contents were tested to failure and produced results that demonstrated the enhancement in punching shear capacity achieved with the addition of fibers. The authors proposed an equation of the same form as the ACI 318-02 [7] code equation for punching shear, but modified it to account for the fiber contribution. The equation proposed is

$$V_{uf} = [\,(0.3\,W_f - 6.8\,)\,(\sqrt{f'_c}/1000)\,(b_o\,d) \quad (kips) \tag{4}$$

where W_f percent of fibers by weight of concrete (%), f'_c concrete compressive strength (psi), b_o critical perimeter at defined by ACI (in), and d average effective depth to tension reinforcement (in).

ACI 318M-02 Equation by J. B. De Hanai and K. M. A. Holanda 2008 [24]

The ACI 318M-02 [7] by J. B. De Hanai and K. M. A. Holanda 2008 [9] adopts a relation between concrete tensile strength (split test) and the square root of the compressive strength, as shown in equation (5).

$$f_{sp} = 0.5563\,\sqrt{f_c} \tag{5}$$

Being f_c the concrete strength to axial compression and f_{sp} the concrete tensile strength (split test), both in MPa. Many authors demonstrate a strong correlation between shear strength and the square root of concrete compressive strength. This corresponds to an indirect correlation of shear strength to the concrete tensile strength. It is well known that when al low volume fraction of steel fibers are added to concrete, the first cracking strength is not significantly increased. However, ductility and post cracking resistance can be increased, thus providing shear resistance by bridging diagonal cracks. In addition, because fibers would control the opening of these cracks, shear resistance through aggregate interlock would likely be increased. Equation (5) from ACI code is very simple and affordable for practical calculations. Therefore, a tentative analysis was done to verify if it also is able to represent by means of a single parameter, the tensile strength of fiber reinforced concrete, the shear load capacity increase in situations of diagonal tension rupture. At first, to correlate the concrete tensile strength to the compressive strength of the steel fiber reinforced concrete, a linear regression of experimental results was made. Equation (6) express this relationship in a similar format of (5).

$$f_{sp} = (0.19\ V_f + 0.53)\ \sqrt{f_c} \quad (6)$$

being f_{sp} and f_c given in MPa and V_f in %. The ACI 318M-02 [12] prescribes (7) to evaluate the ultimate punching load for slabs without transversal reinforcement and square section slabs.

$$V_{uf} = (0.3321\ \sqrt{f_c}\ b_o\ d)/10 \quad (7)$$

where f_c concrete axial compressive strength, $b_o = 4(c+d)$ perimeter where punching occurs, d effective slab depth, and c slab length, being f_c given in MPa, and b_o , d in cm. The value of f_{sp} from (6) is introduced in (7) to consider the effect of steel fibers in punching strength. Adaptations were done to preserve the adjustment and safety factors that are implicit in the coefficient 0.3321 of (7). By this procedure (9) was obtained.

$$V_{uf} = [(0.3321/0.53)\ (0.19\ V_f + 0.53)\ \sqrt{f_c}\ b_o\ d]/10 \quad (8)$$

$$V_{uf} = [0.6266(0.19\ V_f + 0.53)\ \sqrt{f_c}\ b_o\ d]/10 \quad (9)$$

Predicate formula

$$V_{uf} = [\ (1.5W_f - 5.8\ )\ (\sqrt{f'_c}/1000)\ (b_o\ d) \quad (kips) \quad (10)$$

where W_f percent of fibers by weight of concrete (%), f'_c concrete compressive strength (psi), b_o critical perimeter at defined by ACI (in), and d average effective depth to tension reinforcement (in).

B. Compared to the Results Obtained during Testing

Table V shows the results obtained during testing from FEM analysis, predict formula and the results obtained from equations ACI 318M-02[7] by J. B. De Hanai and K. M. A. Holanda 2008 [9] and Shaaban and Gusent 1994 [4] As shown in Fig. 23 shows that the theoretical results from Finite Element Analysis indicate in general a good agreement with equation Shaaban and Gusent 1994 [5]. The results of the analysis indicate that the best equation for predicting the punching shear capacity for SFRC slabs is the new predict formula which obtained from this study.

TABLE V
COMPARISON OF RESULTS TO OTHER MODELS

Spec.	F_{cu} (MPa)	V_f (%)	$V_{uExp.}$ (kN)	ACI D&H[2] V_{u1} (kN)	S&G[3] V_{u2} (kN)	F.E.M V_{u3} (kN)	Predict Formula V_{u4} (kN)
S2	64	0.0	270	229.6	386.7	322.5	329.9
S3	55	0.75	313	212.9	358.1	360	304.0
S4	55	1.0	---	213.1	358.0	270	303.3
S5	55	1.5	---	213.2	367.8	315	302.1

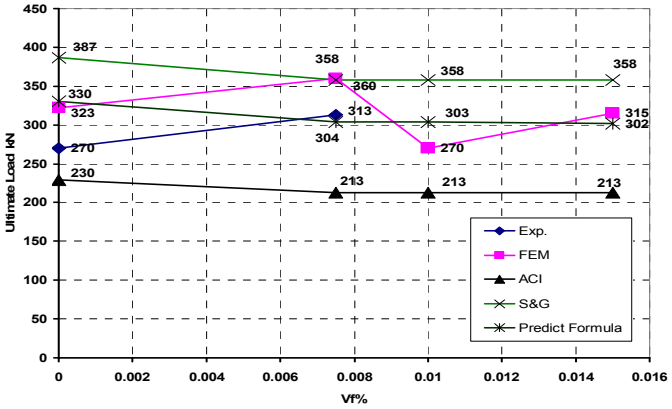

Fig. 23 Comparison of results to other models

IX. CONCLUSIONS

Based on the results obtained from study, the following conclusions can be drawn:

1. The accuracy of the proposed procedure has been well confirmed by the close values of ultimate vertical load, corresponding vertical displacement and peak stresses obtained from the FEM, theoretical, and the experimental results.
2. Using steel fibers with volume fraction equal to 0.75% with self compacted concrete is the ideal percentage used and this percentage increase the punching shear resistance of the slabs by 15%
3. Using steel fibers with volume fraction greater than 0.75% with self compacted concrete leads to decrease the ultimate vertical load and decrease the corresponding vertical displacement.
4. Increasing of flexural reinforcement (lower steel, tension steel) with percentage 40% has slightly effect on the behavior of slab where increase on the ultimate load slab with percentage 3%.
5. Increasing of the upper steel (compression steel) with percentage 40% has significant effect on the behavior of slab where increase on the ultimate load slab with percentage 10%.
6. Theoretical analysis based on Shaaban and Gusent 1994 [5], adapted to steel fiber reinforced concrete provided good indicators of punching shear strength of slabs and good agreement with the FEM results.
7. A new general formula was predicted from this study, which was given results close to FEM and Shaaban and Gusent 1994 [5] . The equation proposed is

$$V_{uf} = [\ (1.5W_f - 5.8\ )\ (\sqrt{f'_c}/1000)\ (b_o\ d) \quad (kips)$$

where W_f percent of fibers by weight of concrete (%), f'_c concrete compressive strength (psi), b_o critical perimeter at defined by ACI (in),and d average effective depth to tension reinforcement(in).

8. Finally, It was observed that the results obtained from ANSYS finite element program are considerably correlated to the results of the experiment. This shows

that the modelings that are made with ANSYS finite element program give us reliable results similar to the previous reports in the literature. In conclusion the modelings that are made with ANSYS finite element program can be useful for saving money and time in terms of the specimen. Also, the design errors which can be made in the design stage or wrong material selection can be prevented. The author believes that this way of modeling will be a guide for the further experimental studies.

REFERENCES

[1] ANSYS User's Manual, Swanson Analysis Systems, Inc 10. William, K.J. and E.D. Warnke (1975) "Constitutive model for the triaxial behavior of concrete". Proceedings of the International Association for Bridge and Structural Engineering.

[2] Alexander SDB and Simmonds SH (1992). Punching shear tests of concrete slab-slab joints containing fiber reinforcement. ACI Structural Journal. 89(4), pp. 425-432 .

[3] Theodorakopoulos D.D., Swamy N. Contributions of steel fibers to the strength characteristics of lightweight concrete slab-slab connections failing in punching shear. ACI Structural Journal 1993;90(4):342-355 .

[4] Shaaban AM and Gesund H (1994). Punching shear strength of steel fibers reinforced concrete flat plates. ACI Structural Journal. 91(3), pp. 406-414 .

[5] Harajli MH, Maalouf D, and Khatib H (1995). Effect of fibers on the punching shear strength of slab-slab connections. Cement & Concrete Composites. 17, pp.161-170 .

[6] McHarg PJ, Cook WD, Mitchell D, and Young-Soo Y (2000). Benefits of concentrated slab reinforcement and steel fibers on performance of slab-slab connections. ACI Structural Journal. 97(2), pp. 225-234 .

[7] ACI 318M-02. Building code requirements for structural concrete. American Concrete Institute, Farmington Hills, Michigan, 2002.

[8] Naaman AE, Likhitruangsilp V, and Parra-Montesinos GJ (2007). Punching shear response of high-performance fiber-reinforced cementitious composite slabs. ACI Structural Journal. 104(2), pp. 170-1779

[9] De Hanai, J.B. and Holanda , K.M.A." Similarities between punching and shear strength of steel fiber reinforced concrete (SFRC) slabs and beams" IBRACON Structures and Materials Journal vol. 1, No. 1, 2008

[10] Meisam Safari Gorji (2009) "Analysis of FRP Strengthened Reinforced Concrete Beams Using Energy Variation Method" World Applied Sciences Journal 6 (1): 105- 111.

[11] Cheng MY and Parra-Montesinos GJ (2010a). Evaluation steel fibers reinforcement for punching shear resistance in slab-slab connections-part1: Monotonically increased load. ACI Structural Journal. 107(1), pp. 101-109